

# Dependence of the cooling force on the electron transverse velocity

Fermilab PARTI 2010 Summer Internship Report

Andrei Khilkevich, Belarusian State University, Minsk, Belarus

Supervisor: Lionel R. Prost, Fermilab, Batavia, IL, USA

## Introduction

Recently, an interest to run the Relativistic Heavy Ion Collider (RHIC) at low beam total energies of 2.5-25 GeV/nucleon [0] has emerged in order to probe the existence and location of a critical point on the quantum chromodynamics (QCD) phase diagram. To achieve the physics goals in a timely manner, the luminosity lifetime would have to be increased with respect to what it is believed can be achieved currently. It is perceived that a possible solution would be the use of electron cooling, which would counteract intra-beam scattering (IBS), hence significantly increase the average luminosity. On the other hand, in the cooling section, the interaction of the ion and electron beams results in ion beam loss due to recombination. In a paper presented at PAC 2007 [1], it was suggested that ion recombination could be greatly reduced by a coherent oscillatory motion of the electron beam (achieved with a relatively weak undulator field), while the accompanied degradation of the cooling efficiency would remain modest. However, this idea was never tested before experimentally and in this paper, we present an attempt to quantify the impact of the undulatory motion on the friction force (or also called cooling force).

In Fermilab's electron cooler, a 0.1A, 4.3MeV DC electron beam is used to cool 8.9 GeV antiprotons stored in the Recycler Ring (RR). In part, the beam propagates through a 20m long 'cooling section', which consists of 10 identical modules. Each module comprises a 2 meter long solenoid, 20 dipole correctors and a Beam Position Monitor (BPM) at its beginning. The correctors are used to compensate the magnetic field imperfections. However, these correctors can also be used to create a helix-like trajectory of the electron beam with a wave length of 1 - 10 m, therefore mimic the trajectories obtained with an undulator and permit studying the dependence of the longitudinal cooling force on the value of the added transverse electron velocities that results from these oscillations. In addition to measurements of the cooling force for several oscillation wavelengths, we compare these data with a model, in which the cooling force is calculated as a sum of "near" and "far" non-magnetized collisions [6].

## Electron cooling and Fermilab cooling section

Electron cooling is a method to decrease the 6D phase space of charged particle beams without any loss of particles, at least from the method itself. The idea of electron cooling is rather old. It first was suggested by G.I. Budker in 1966. The principle can be described with the analogy of mixing hot and cold gases. As a result of the gas molecules interaction, the temperature of the hot gas will decrease and the temperature of the cold gas will correspondingly increase. In other words, through collisions, molecules with high velocities (hot gas) transfer some of their energy to molecules with low velocities (cold gas) until an equilibrium is reached and the average velocity of all the molecules are the same. For electron cooling, the transfer of energy between the hot particles (the beam to be cooled) and the cold particles (the electron beam) is the result of Coulomb collisions. At Fermilab the particles to be cooled are antiprotons.

A circulating beam of hot antiprotons is combined over a certain length of the Recycler with a well directed electron beam, which spread of energy is also very low. The cooling happens in the following way: the electrons are accelerated to the point, where they match the mean longitudinal velocity as the antiprotons. Then both beams interact for a certain length and in the end the electron beam is removed. The section where the beams are combined is called a cooling section and its overview is given below.

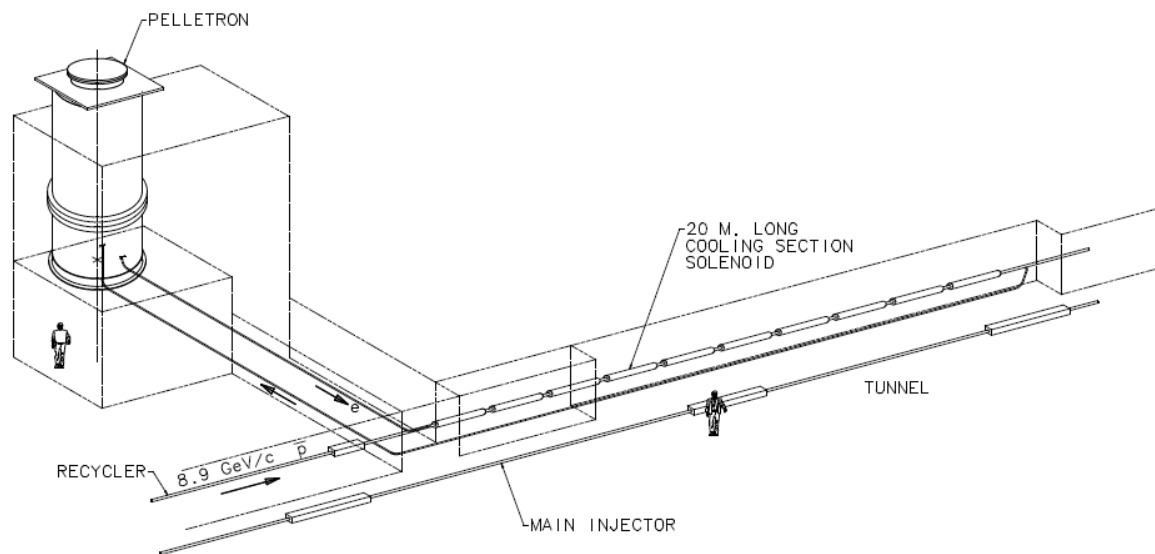


Figure 1. General layout of the Recycler electron cooler.

The electron beam is generated with the Van de Graaff-like accelerator, called Pelletron. The beam energy at the exit of the Pelletron is 4.3 MeV, so that the relativistic  $\gamma$ -factor of the electrons match the one from the  $8.9 \text{ GeV}/c$  antiproton circulating. Then, it is

transported to the cooling section, which is approximately 20 meters long. After interacting with antiprotons in that section, the electron beam makes a U-bend and returns eventually to the Pelletron, where it is decelerated and recuperated in the collector. This is the so-called recirculation mode. Inside of the cooling section solenoids create a constant longitudinal magnetic field, which equals to  $\sim 100$  G.

## Implementation of the Helical Trajectories

The purpose of the longitudinal magnetic field inside the cooling section is to focus the electron beam so that trajectories remain parallel. As it was mentioned before, in each of the 10 modules in the cooling section, there are 20 correctors. The nominal values of the currents for these correctors are chosen so that the transverse magnetic field component is minimized. In order to obtain an undulatory trajectory, corrector currents are adjusted such that, the beam will be kicked by each corrector in a certain direction and with a certain amplitude, so that the beam three-dimensional trajectory be close to a helix with period  $\lambda$  in the Z direction (longitudinal) and an amplitude  $A_x$  and  $A_y$ , in the X and Y directions, respectively. Note that ideally,  $A_x$  and  $A_y$  are equal. A program based on the derivation and equations from [2] was composed to numerically calculate the beam trajectories. This calculates the theoretical trajectory of the electron beam inside the cooling section, and modifies the values of the corrector currents until the difference between the calculated trajectory and the desired undulatory trajectory is minimal.

With this method, helix-like trajectories with four different periods were created:  $\lambda = 1\text{m}$ ,  $2\text{m}$ ,  $4\text{m}$  and  $6\text{m}$ . The "natural"  $13\text{m}$  period due to the presence of the longitudinal magnetic field in the cooling section (and associated Larmor rotation) was used as an additional data point. To test the accuracy of the electron beam trajectories obtained with this method, its position was recorded with the cooling section BPMs for the case  $\lambda = 4\text{m}$ , which corresponds to half an oscillation per module. Thus, the readings of all the BPMs of the X coordinate should give zero and Y coordinate readings should have the same magnitude but with opposite signs between two adjacent BPMs.

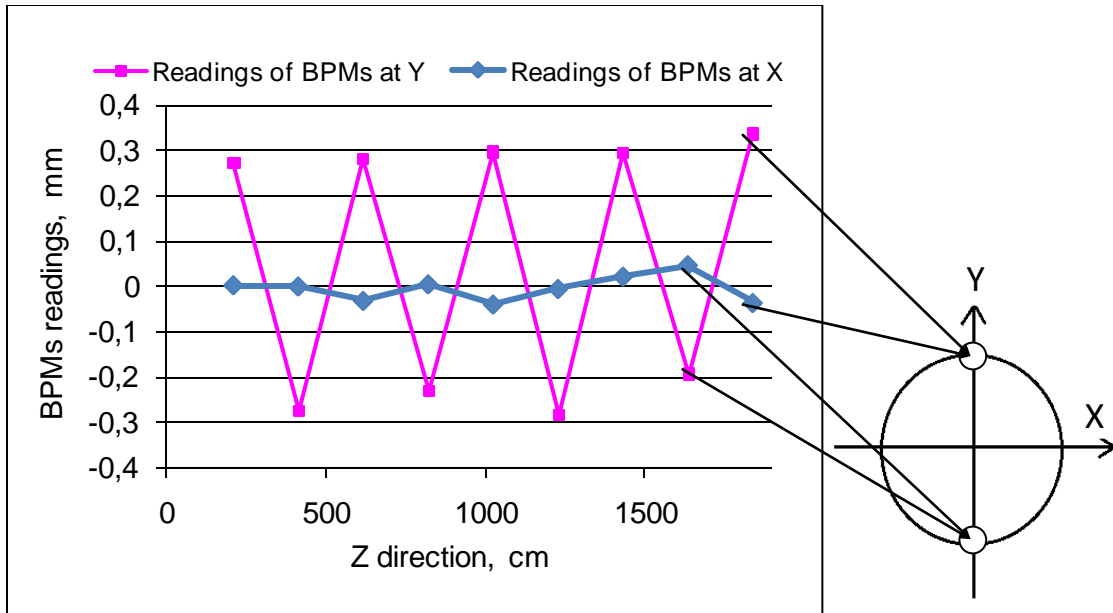


Figure 2. BPMs readings for  $\lambda = 4\text{m}$ . The diagram on the right represents the beam trajectory in the plane perpendicular to the beam propagation direction (X-Y plane)

Figure 2 shows that there is a fairly good agreement between the actual trajectory of the beam and the ideal calculated trajectory. The limitation in implementing oscillations of different amplitudes in the experiment was that the maximum values of currents in correctors should not exceed the critical for work values with the increase of undulatory angle  $\alpha_{\text{und}}$  (see below). Obtained solutions allowed to take the data till:

$$\alpha_{\text{und\_max}} = 0.5\text{mrad for periods of 2m and 6m}$$

$$\alpha_{\text{und\_max}} = 0.4\text{mrad for periods of 1m and 4m}$$

## Measurements Method

Several series of measurements were performed on April 27<sup>th</sup>, July 13<sup>th</sup> and July 17<sup>th</sup>, 2010. Current values obtained with the were applied to the correctors using the so-called ‘Wave Generator’ Java application. Another Java application, Autotune, ensures that the initial conditions for the beam entering the cooling section remain constant. The method we employed to measure the cooling force experimentally is the so-called “voltage jump” method [3]. The typical number of antiprotons was small ( $1-2 \times 10^{10}$ ) and we started by making a coasting beam (no RF structure) that filled the entire Recycler ring (longitudinally) and had a small transverse emittance. Then, the beam was cooled to an equilibrium state with the electron beam. Finally, the electron beam energy was changed instantaneously by 2 keV (at this time, the transverse stochastic cooling system was turned

off and remained so for the duration of the measurement). The electron cooling force dragged the antiproton longitudinal distribution to this new equilibrium momentum which is  $M_p/m_e$  times the voltage jump away from the initial equilibrium. The energy jump was kept every time for 2 minutes to make sure that the number of points for determining the drag-rate was enough. Using the data logger from ACNET (Fermilab controls system), we determined for every experimental point the exact time when the voltage jump occurred and ended, and plotted the dependence of the pbar momentum deviation as a function of the time during the period of the voltage jump (see Figure 3). The value of the mean longitudinal cooling force is by definition the slope of the linear fit to  $P(t)$ , where  $P$  is the average momentum of the antiproton beam. Applying such fits to every measurement in all series of experiments, we found the standard errors of fits, and therefore the statistical error for every point of the cooling force value. For all plots with data points below, the error-bars include only the statistical error. Other kinds of errors that could contribute to the overall cooling force uncertainty are:

1) The uncertainty of choosing the initial and final points of the pbar momentum deviation to fit. However, the analyses of the fits show that the contribution of this source of error is rather weak compared to the statistical one.

2) The uncertainty of the pbar emittance.

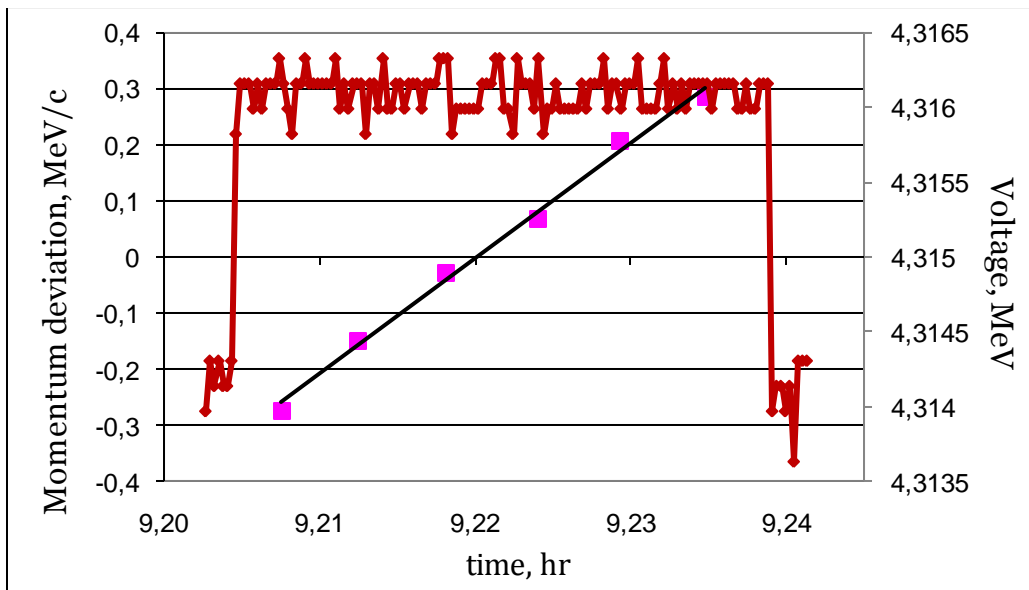


Figure 3. Red points indicate the voltage jump during the measurements; pink squares – the pbars momentum deviation with respect to the Recycler Ring nominal momentum.

## Theoretical Model

Previous studies [4] indicate that without undulations the cooling force in Fermilab cooling section could be successfully described with a classical non-magnetized model. We believe that the helix-like motion should not significantly change the way the pbar and electron beams interact, and therefore mere modifications to the non-magnetized model could be used in this particular case. A justification for this statement is that the maximum undulation amplitude used in the experiments was 0.5 mm, while the electron beam radius is near 1.8 mm.

The non-magnetized model mentioned above describes the average force acting on a single antiproton from the electron beam. For this model to be valid when comparing the calculated value of the cooling force to the drag-rate measurements, the number of pbar was kept small ( $1-2 \times 10^{10}$ ), so the pbar beam was pencil-like. The interaction of the pbar with the electron beam accounts the impact parameters going from minimal  $\rho_{min}$  to the maximum  $\rho_{max}$ . The minimal impact parameter is chosen such the scattering angle is  $90^\circ$ :

$$\rho_{min} = r_e \frac{c^2}{|\vec{V}_p - \vec{V}_e|^2} \quad (1)$$

where:

$r_e$  – electron classical radius;  $\vec{V}_p$  – the velocity of the pbar beam;

$V_e$  – the velocity of the electron beam;

while the maximum impact parameter is chosen as Debye shielding radius.

The non-magnetized model is based on the following assumptions: collisions are assumed to be binary and complete; the electrons velocity spread is described by a Gaussian distribution; the Coulomb logarithm is assumed to be independent from the relative velocity of the beams;  $\rho_{max} \gg \rho_{min}$ . By applying this model to the Fermilab cooling section, we assume that the influence of the longitudinal magnetic field on cooling can be neglected. Under these assumptions the cooling force is calculated by the classical formula [5]:

$$\mathbf{F} = 4\pi n_e m_e r_e^2 c^4 \eta L_c \int_{-\infty}^{+\infty} \frac{\mathbf{V}_p - \mathbf{V}_e}{|V_p - V_e|^3} f(V_e) d^3 V_e \quad (2)$$

where:

$n_e$  – electron density in beam rest frame;  $m_e$  – electron mass;

$r_e$  – electron classical radius;  $\eta$  – ratio of ring length occupied by cooling section

to the Recycler ring circumference;  $V_p$  – the velocity of the pbar beam;

$V_e$  – the velocity of the electron beam;  $L_c = \frac{\rho_{max}}{\rho_{min}}$  – Coulomb logarithm;

In the non-magnetized case the electron beam is assumed to move along the straight line. When the undulations are applied, however, the electron beam centroid moves along an helicoidally trajectory. Such a type of motion effectively introduces an additional coherent transverse velocity  $U_{und}$  to the straight motion assumed in the non-magnetized model. For the description of the transverse velocity spread, an angle  $\alpha$  is usually introduced. It can be defined as:

$$\alpha = \frac{V_t}{\gamma\beta c} \quad (3)$$

where:  $V_t$  is rms transverse velocity spread of the electrons.

It should be mentioned that due to the non-ideal magnetic field and other imperfections in the cooling section as a whole, the angle  $\alpha$  is not equal to zero even when no undulation is applied. We will denote such "zero" angle as  $\alpha_0$ . The measurements show that it is  $\sim 0.1$  mrad.

Similarly, the additional angle  $\alpha_{und}$  due to the undulatory trajectories can be defined as:

$$\alpha_{und} = \frac{2\pi\rho_{und}}{\lambda} \quad (4)$$

where:  $\rho_{und}$  – the undulation amplitude;  $\lambda$  – the period of undulation;

So, when undulations are applied, the electron beam moves in the transverse plane along circles of radius  $\rho_{und}$ :

$$\rho_{und} = \frac{U_{und}}{\gamma\beta c} \frac{\lambda}{2\pi} \quad (5)$$

In the presence of the undulatory motion, the collisions could be divided into two parts according to the value of the impact parameter [6]. The collisions with small impact parameters are affected by the circular motion, which essentially increases the transverse velocity. On the other hand, for impact parameters significantly larger than the rotation radius, the effect of additional rotation will be negligible. The choice of the boundary impact parameter which separates these two areas is to some extent arbitrary due to the rough separation of the areas in the model itself. In this paper, the boundary impact parameter is chosen to be equal to  $\rho_{und}$ , as in [1]. So, the two contributions to the cooling force in the electron beam frame during a drag rate measurement are defined as:

$$F_{NC,Z} = 4\pi n_e m_e r_e^2 c^4 \eta \iiint_{-\infty}^{+\infty} \frac{\log\left(\sqrt{\frac{\rho_{und}^2 + \rho_{min}^2}{\rho_{min}^2}}\right) (V_z + \Delta V_z) f(V_e)}{\left|(V_x)^2 + (V_y + U_{und})^2 + (V_z + \Delta V_z)^2\right|^{3/2}} dV_x dV_y dV_z \quad (6)$$

and

$$F_{FC,Z} = 4\pi n_e m_e r_e^2 c^4 \eta \iiint_{-\infty}^{+\infty} \frac{\log\left(\sqrt{\frac{\rho_{und}^2 + \rho_{max}^2}{\rho_{und}^2 + \rho_{min}^2}}\right) (V_z + \Delta V_z) f(V_e)}{\left|(V_x)^2 + (V_y)^2 + (V_z + \Delta V_z)^2\right|^{3/2}} dV_x dV_y dV_z \quad (7)$$

with

$$f(V_e) = \frac{1}{(2\pi)^{\frac{3}{2}} \sigma_x \sigma_y \sigma_z} e^{-\left(\frac{V_x^2}{2\sigma_x^2} + \frac{V_y^2}{2\sigma_y^2} + \frac{V_z^2}{2\sigma_z^2}\right)} \quad (8)$$

where:

$\Delta V_z$  – electron velocity increase due to the voltage jump;

$\sigma_x, \sigma_y, \sigma_z$  – rms transverse velocity spread on X, Y and Z axis respectively;

The mentioned above angle  $\alpha_0$  determines the electron velocity spread  $\sigma_x$  and  $\sigma_y$  by :

$$\alpha_0 = \frac{\sigma_t}{\gamma\beta c} \quad (9)$$

and

$$\sigma_x = \sigma_y = \frac{\sigma_t}{\sqrt{2}} \quad (10)$$

The longitudinal velocity spread  $\sigma_z$  is assumed to be present only because of the noise in the voltage jump.

Then, the total value of the longitudinal cooling force  $F_z$  is the sum of the force due to *near collisions*,  $F_{NC,Z}$ , and *far collisions*,  $F_{FC,Z}$  :

$$F_z = F_{NC,Z} + F_{FC,Z} \quad (11)$$

The contribution of each part is illustrated on the following plot:

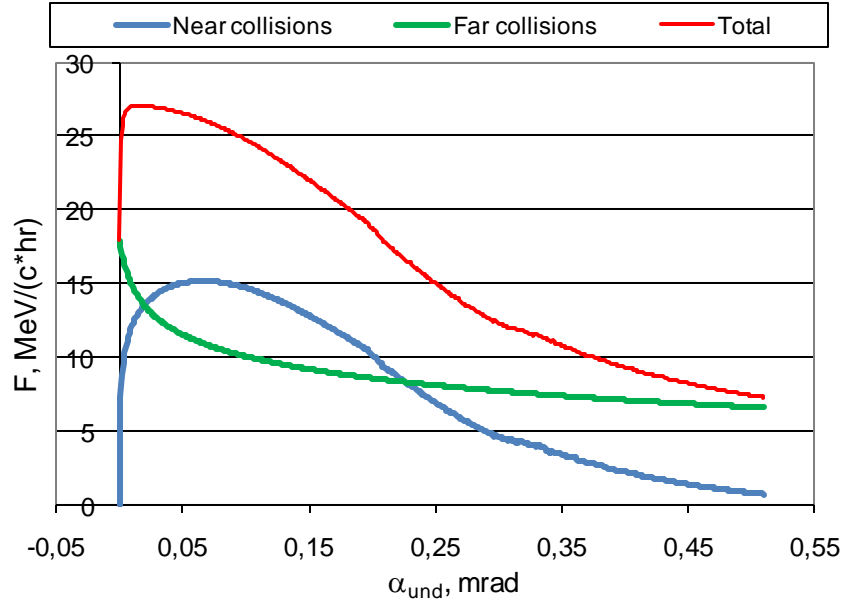


Figure 4. Dependence of the  $F_{NC,Z}$ ,  $F_{FC,Z}$  and  $F_z$  on the undulatory angle. Simulation is for  $\alpha_0 = 1.4$  mrad,  $\lambda = 6$  m,  $\sigma_x = \sigma_y = 4.0 * 10^5 \frac{m}{s}$ ,  $\sigma_z = 2.2 * 10^4 \frac{m}{s}$ .

## Results

From the measurements, the dependence of the cooling force on the undulatory angle  $\alpha_{und}$  was established. However, while the increase of the undulatory angle is equivalent to the increase of the undulation amplitude for a fixed period (Eq. 3), it also results in a constant offset of the electron beam with respect to the Z axis (*i.e.* the radius of the circle shown on Figure 3). Such a change of the offset implies that the pbar beam interacts with different parts of the electron beam, and since the electron beam density is not uniform along the transverse directions, the offset contributes to (decreases) the overall value of the cooling force which is measured for a constant undulatory angle. As this paper is devoted to the study of the dependence of the cooling force with respect to the undulatory angle, the data needed to be processed such that only its contribution would be taken into account.

For this purpose, the data from drag-rate measurements with different beam offsets [7] was used.

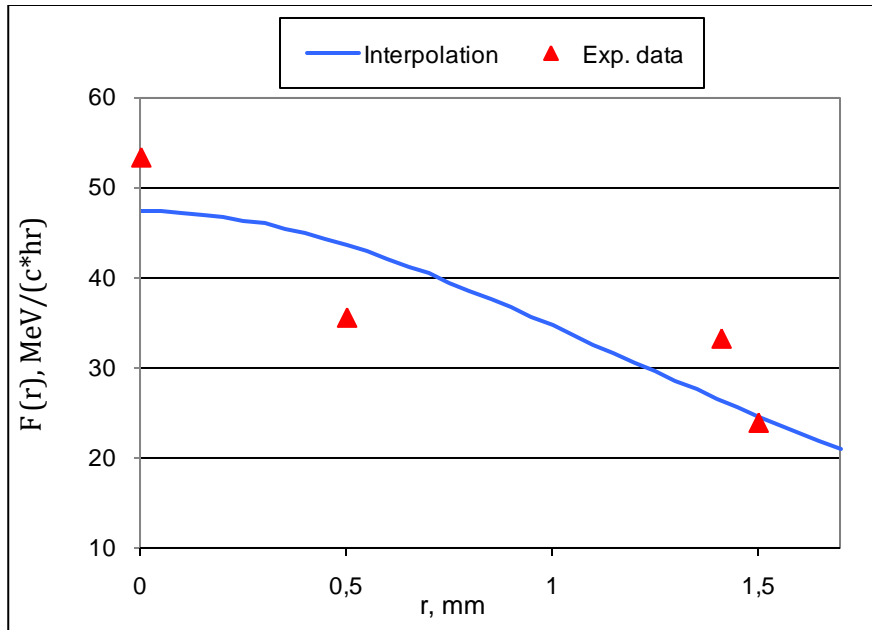


Figure 5. Dependence of the cooling force on the electron beam offset.

In our case, the maximum beam offset was about 0.5 mm, so its contribution to the decrease of the total cooling force according to Figure 4 should be on the order of 10% (using the interpolation curve). As an example, the effect from the beam offset is shown on Figure 6.

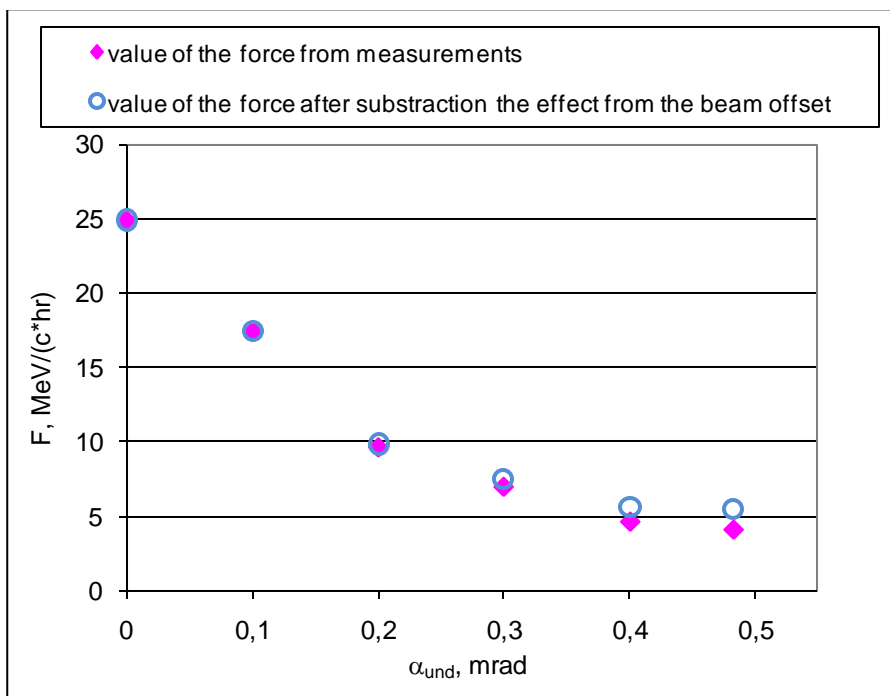


Figure 6. Dependence of the cooling force on the undulatory angle with and without taking into account the effect from the beam offset.

Figure 6 shows that the contribution from the beam offset becomes significant only for the undulatory angles  $\alpha_{und} \geq 0.4$  mrad. After this procedure was applied to all data, the cooling rate as a function of the undulatory angle only for all measurements was obtained and plotted on Figure 7.

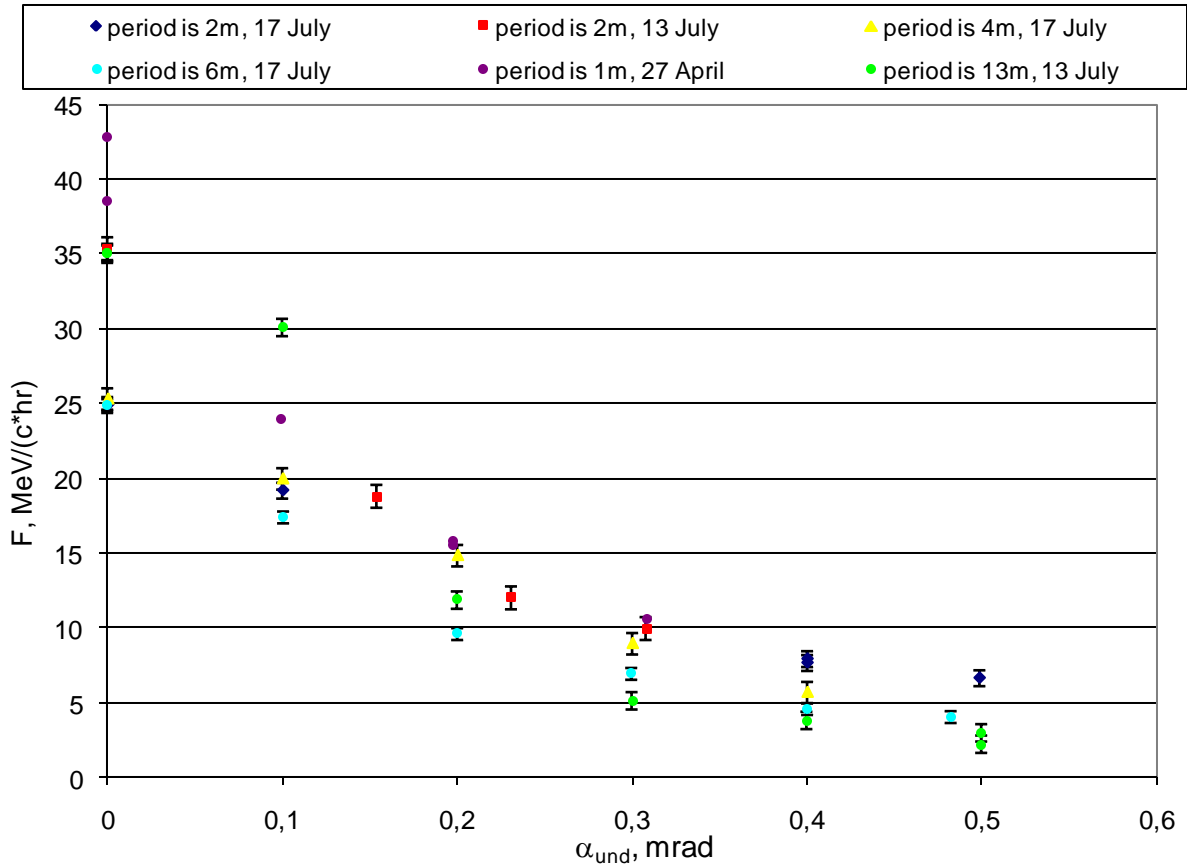


Figure 7. Dependence of the cooling force on the undulatory angle for all series of data. Error bars represent the statistical errors.

The first observation is that there are large inconsistencies in the measurements taken on different days, even for zero undulatory angle. The difference is the largest between the data points taken on July 17<sup>th</sup> 2010 and the other data points. One possible explanation may be that it comes from recalibrating the BPMs. Because of the specifics of tuning the beam position and angle at the entrance of the first module of the cooling Ssection (namely, the beam position in the first two BPM is always kept on axis) an additional coherent angle inside the cooling section could result. Therefore, in order to compare the data to the model (Eqs. 4-8,11) over the full scale of  $\alpha_{und}$ , we only used the

data points taken on one day (July 13<sup>th</sup> 2010). Results for  $\lambda = 2\text{ m}$  and  $13\text{ m}$  (minimum and maximum at that day, respectively) are plotted on Figure 8.

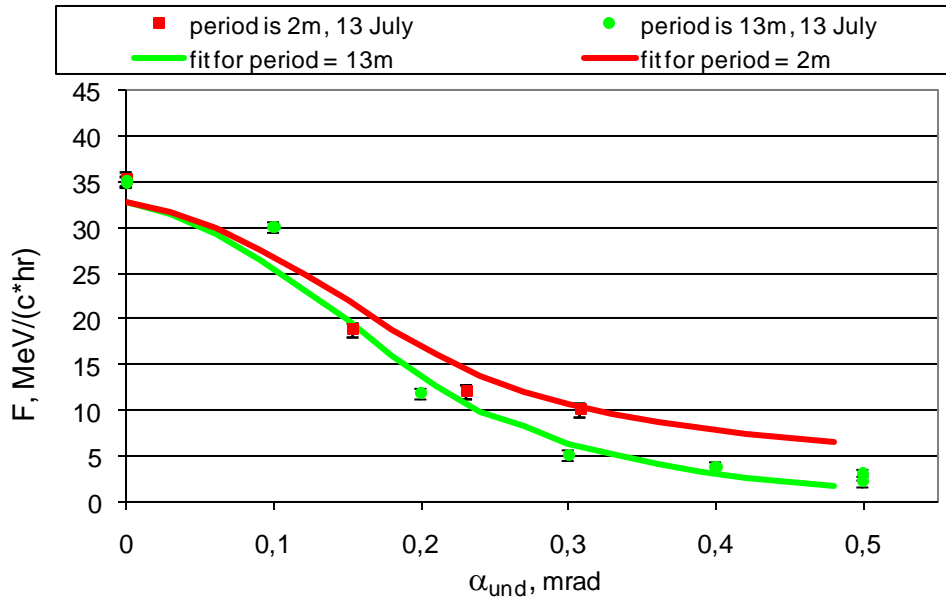
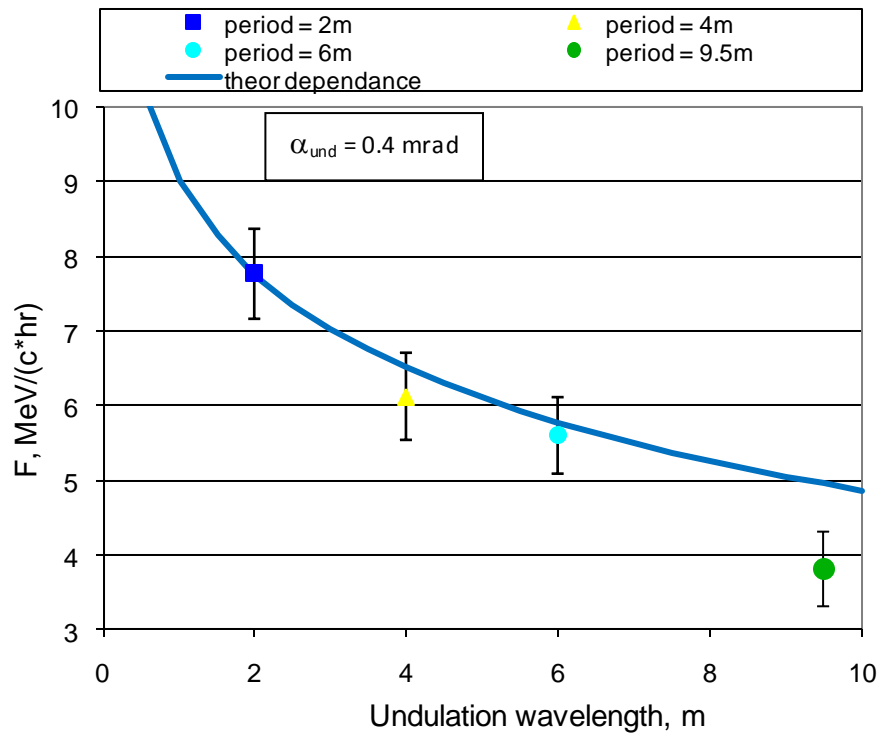
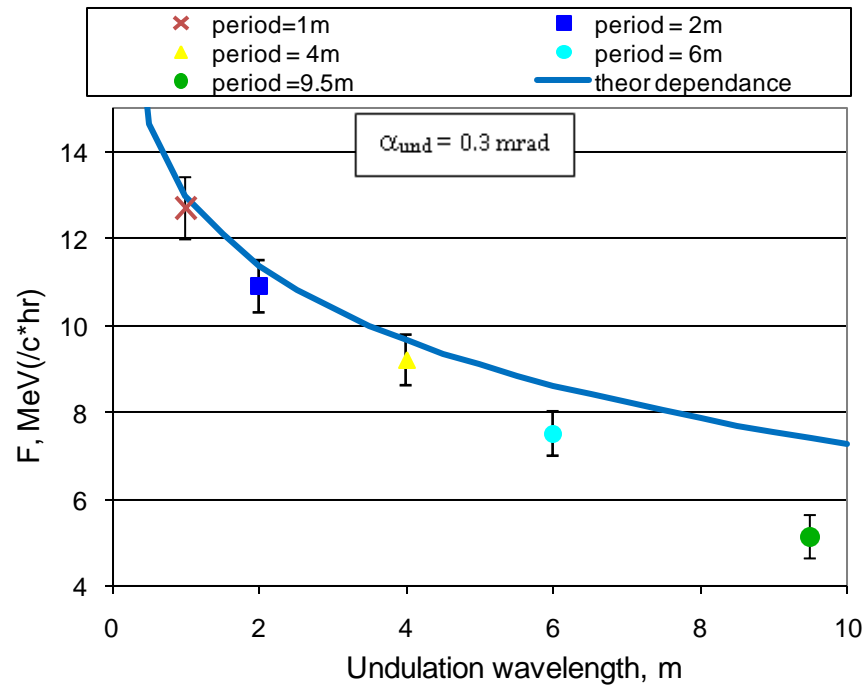
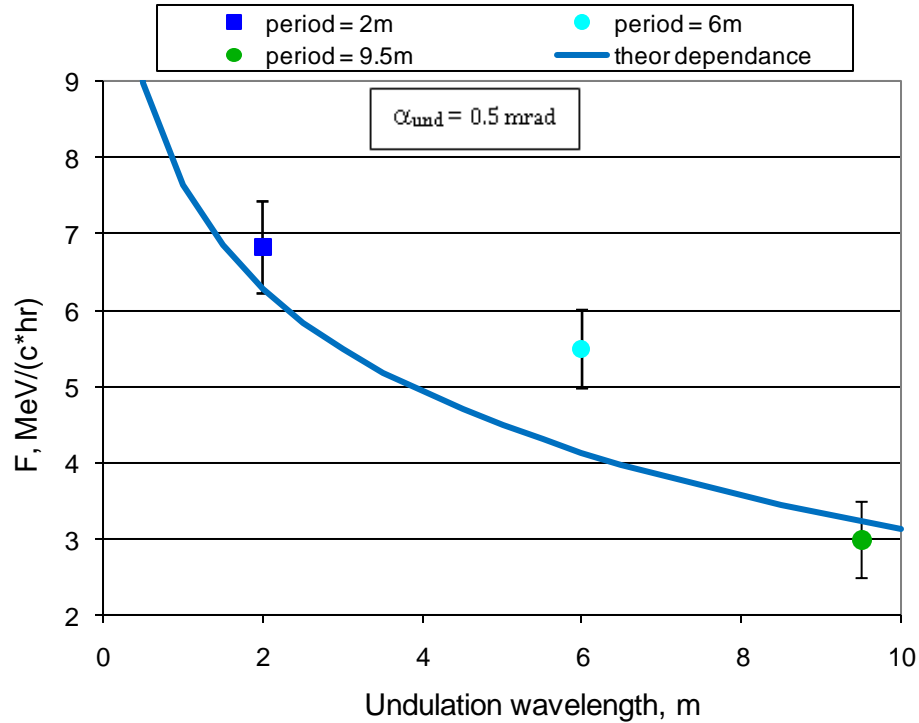


Figure 8. Dependence of cooling force on the undulatory angle and comparison to the theory prediction. Fits are made for:  $\alpha_0 = 0.11\text{ mrad}$ .

The theoretical model was found to predict well the general behavior of the measured cooling force as a function of the undulatory angle (or wavelength).

The discrepancies between the data taken on different days shown in Figure 7 bring the question of how they can be compared fairly. The influence of  $\alpha_0$  is large for undulatory angles  $\alpha_{und} < \alpha_0$ , but when  $\alpha_{und}$  increases, the influence of  $\alpha_0$  on the cooling force is reduced. Therefore, data points from different days taken at large  $\alpha_{und}$  should still be valid for direct comparison. Then, the cooling force as a function of the oscillation period for a given  $\alpha_{und}$ , can be plotted (Figure 9).





Figures 9. Dependences of the electron cooling force on the period of oscillations for several undulatory angles.

Once again, the measurements are in fairly good agreement with the model.

## Conclusion

The dependence of the longitudinal cooling force on the angle resulting from coherent oscillations of various wavelengths was studied. The model which assumes that the total cooling force is calculated as a sum of "near" and "far" non-magnetized collisions qualitatively agrees with the experimental data. In the range of undulatory angles where we believe the measurements should be valid for comparison ( $\alpha_{und} \gtrsim 0.3$  mrad), the model predictions of the dependence of the cooling force on the undulation period coincide with experimental dependence with an accuracy of  $\sim 30\%$ .

## Acknowledgment

I want to thank A. Shemyakin for many useful discussions and suggestions, without which the work reported in this paper would not be possible.

## References:

- [1] A. Fedotov *et al.*, PAC07, proceedings THPAS092
- [2] Sergei Seletskiy, FERMILAB-THESIS-2005-59
- [3] H. Danared *et al.*, Phys. Rev. Lett. **72** (1994) 3775
- [4] A. Shemyakin, Beams-doc#2601-v3, 2007
- [5] Ya.S. Derbenev and A.N. Skrinsky, Particle Accelerators **8** (1977), 1
- [6] A.V. Sobol *et al.*, New Journal of Physics **12** 093038 (2010)
- [7] A. Shemyakin *et al.*, EPAC'06 Proceedings TUPLS069